

# Formation Control and Obstacle Avoidance of Multiple Rectangular Agents with Limited Communication Ranges

Thang Nguyen, Hung Manh La, Tuan Dzung Le and Mohammad Jafari

**Abstract**—Formation control of multiple agents has attracted many robotic and control researchers recently because of its potential applications in various fields. This paper presents a novel approach to the formation control and obstacle avoidance of multiple rectangular agents with limited communication ranges. The distributed control algorithm is designed by utilizing an artificial potential function. The convergence and stability analysis of the proposed control algorithm is given. The proposed control algorithm can guarantee fast formation performance and no collision among agents. Also, by proposing a potential repulsive function and utilizing it as an obstacle avoidance function, rectangular agents can perfectly avoid obstacles with different shapes and sizes. As a result, the rectangular agents can move together and quickly form a pre-defined shape of formation such as straight line, circle and lattice, etc., while avoiding the obstacles. Simulation results are conducted to demonstrate the effectiveness of the proposed algorithm.

**Index Terms**—Rectangular agents, Multi-agent systems, Formation control, Network control.

## I. INTRODUCTION

### A. Motivation

Formation control of multi-agent [1], [2] has gained significant interest because of its potential applications in various fields such as target tracking [3]–[7], environmental monitoring [8]–[10], scalar field mapping [11]–[14], intelligent transportation systems [15], etc. The multi-agent networks are combined from sensors, control algorithms and other dynamic factors which depend on specific purpose or application scenarios [1], [4], [14].

There are both centralized and decentralized approaches to the multi-agent formation control. The centralized approach [16] relies on a single controller to generate a free collision avoidance strategy for agents, while the decentralized approach [17]–[19] tried to seek an independent controller to allow each agent to work collaboratively with its neighbors to form a network and avoid collision.

This work was partially supported by the University of Nevada at Reno and the National Science Foundation under the grant: NSF-NRI-1426828.

Thang Nguyen is with Department of Electrical Engineering and Computer Science, Cleveland State University, Cleveland, OH 44115-2214. Email: t.nguyen13@csuohio.edu.

Hung La, Tuan Le and Mohammad Jafari are with the Department of Computer Science and Engineering, University of Nevada, Reno, NV 89557, USA. Corresponding author: Hung La, email: hla@unr.edu

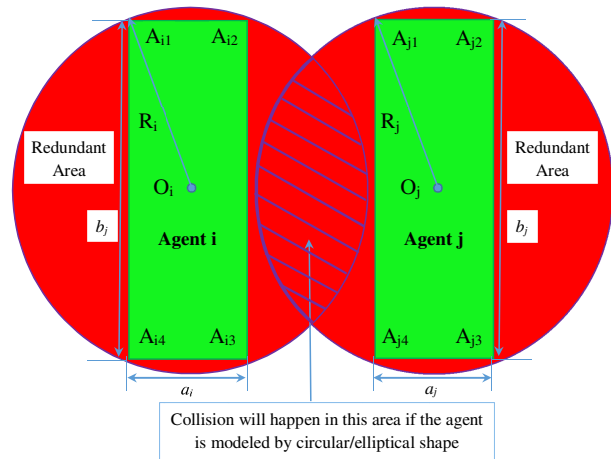


Fig. 1. Illustration of redundant areas of the circular agent when fitting with rectangular agent.

Both centralized and decentralized approaches for multi-agent formation control mainly model agents as circular or elliptical shapes [17], [18], [20]–[27]. However, in practice, many agents have long and narrow shape (Fig. 1) such as rectangular shape like cars or ships, and the existing formation control algorithms for circular or elliptical agents may not be suitable [10], [17], [18], [21], [26], [28]–[31]. In this paper we propose a distributed control algorithm which can be applied to the problem of formation control for all different sizes of rectangular agents, for example autonomous vehicle control in intelligent transportation systems (see Fig. 2).

Unlike the existing work which model agents as single particle/point or elliptical shapes, we consider an agent as a rectangular shape where all four vertices associated with width and length of the rectangle are taken into account of the formation control design. This rectangular model helps remove redundant areas as illustrated in Figure 1. Circular approximation for long rectangular shapes could result a wrong collision avoidance among agents in the case where the agents have to travel through a narrow environment. For example, autonomous cars have to travel in traffic lanes in the city in rush hours (see Fig. 2). The rectangular agent model can be beneficially applied to formation control of multiple autonomous cars in the future of intelligent transportation systems.

TABLE I  
SUMMARY OF RELATED WORK IN MULTI-AGENT FORMATION CONTROL.

Circular Agent Formation (CAF)	Elliptical Agent Formation (EAF)	Rectangular Agent Formation (RAF)
Both centralized and decentralized formation control for multiple circular agents in complex environments have been developed [16], [17], [20], [24].	Formation control for multiple elliptical agents is investigated [18], [26] to address limitations of circular agent modeling and control	Our paper present a new approach to RAF control with limited communication range. Four vertices associated with width and length of the agent are taken into account of the formation control design.
CAF control is mainly designed for circular/disk agents. The control algorithm can handle both noisy-free and noisy environments. However, the agent is modeled as circular shape. Hence it is not suitable for rectangular agents since the collision may exist among agents due to redundant areas (Fig. 1).	EAF is mainly developed for multiple agents which are modeled as elliptical shapes. Hence it is not appropriate to be applied in formation control of rectangular agents because the collision will happen (see Fig. 1).	This approach utilizes the potential field to design the distributed formation control algorithm. The proposed control algorithm allows multiple rectangular agents to move together without collision. The proposed algorithm allows the agents to form different shapes such as straight line, lattice and circle.

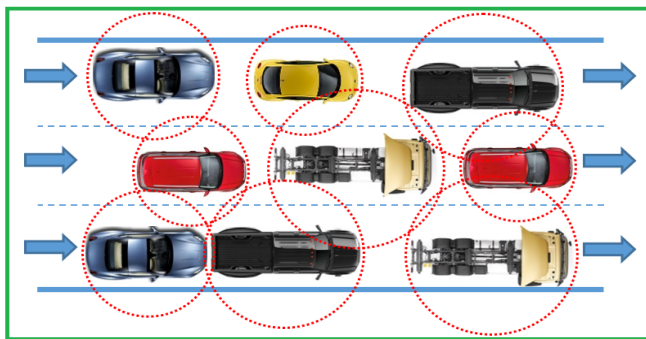


Fig. 2. Illustration of transportation systems with rectangular agents/cars and their circular fit.

Moreover, considering the environment as a free space might not be very practical. The real environment usually contains different types and sizes of obstacles. We proposed an algorithm which could conform the formation while avoiding the different obstacles. For example, it is necessary for autonomous cars to avoid any possible obstacles especially pedestrians while traveling in a city.

### B. Literature Review

Multi-agent distributed control systems have gained increasing interest recently [9], [32]–[35]. Problems of area coverage using multi-agent systems have drawn many interesting studies. Many attentions had been paid to mobile sensing networks due to their flexibility and easy-to-apply to real life applications [36]. In [8]–[10], mobile sensor networks have been deployed for measuring and modeling interested environmental areas. Even though the main purpose of those two studies was to estimate interested areas, without incorporating mobile sensor network for data collection, it would have been extremely hard to have proper estimations. To address the problem of how one should distribute a mobile sensor network into an area, in [34], a statistical approach with Gaussian process has been derived to address the optimization problem of sensor distribution.

Obviously, having a good multi-agent system in the essence of sensing and communications capabilities does not guarantee good area coverages due to dynamic environmental

changes. Cooperative control among agents therefore is essential. Olfati-Saber in [17] provided a general framework for flocking control based on potential field approach. Additionally, many other studies have contributed to this area in which new potential approaches for avoiding local minima problem have been reported in [37], [38]. In [14], a cooperative motion control was combined with consensus filtering to build a map of the scalar field. The popular Kalman filter was incorporated in control strategies due to its efficiency [39]. In [40], a Kalman filter approach has been applied to further improve the cooperative control performance; both cooperative motion control and cooperative sensing were integrated to control the shape of the sensor node formation in order to minimize the estimation errors. In [41], an overview about recent studies on cooperative control for multi-agent systems was provided, in which five categories of cooperative control were defined: consensus, distributed formation, distributed optimization and distributed estimation. In those categories, distributed formation control has been the most attractive topic. For a multi-agent system, formation control is considered as a “general” problem since for its solution, we have to address cooperative control methods and after achieving a formation control technique, we can apply it to area coverage problems. Additional extension to formation control for circular agents in noisy environment has been reported in [22], [23], [25]. To the best of the author’s knowledge, previous studies on aforementioned problems typically considered agents with circular or disk-shapes [20], [24]. The reason for that is it simplifies complex algorithms such as obstacle and/or collision avoidances by not taking into account any real physical shape of an agent in a real application. In [18], [26] the author took a different approach by considering agents with a rectangular shape. However, the author did not fully examine the rectangular shape but instead, fitting those rectangular shaped agents into elliptical disks to reduce the conservative area in comparison with that area by fitting agents into a circular disk.

The main contribution of this paper is to provide a theoretical and computational framework for design and analysis of a distributed formation control algorithm for multiple rectangular agents in presence or lack of obstacles. A new approach to the rectangular agent model is proposed with a

consideration of all four corners/vertices of the agent to avoid redundant areas. This rectangular shape modeling approach can be extended to other shapes with more than 4 vertices. The proposed distributed formation control algorithm can allow rectangular agents to form different formation shapes such as line, lattice or circular shape, respectively. An artificial potential field based approach is utilized in designing the formation control law to enable agents to avoid collision with each other and obstacles. The convergence analysis for the proposed work is given.

The rest of the paper is organized as follows. The next section presents multi-rectangular agent and obstacle models and the associated distance definitions. Section III presents the problem statement of formation control for multiple rectangular agents. Section IV presents our proposed control algorithm for multiple rectangular agents. The simulation results are presented in Section V. The conclusion of the paper is given in Section VI.

## II. PRELIMINARIES

### A. Multi-Rectangular Agent Model

Consider two rectangles  $i$  and  $j$ , where  $(x_i, y_i)$  denotes the position of the center  $O_i$  and  $\phi_i$  is the heading angle of rectangle  $i$  as shown in Figure 3. The length and width of rectangle  $i$  are  $b_i$  and  $a_i$ , respectively (see Fig. 1). Furthermore,  $O_i X_i Y_i$  denotes a coordinate frame associated with agent  $i$ .  $(x_A^i, y_A^i)$  is the coordinate of point  $A$  in the frame  $O_i X_i Y_i$ . The notation for rectangle  $j$  is similar. For brevity,  $c$  and  $s$  stand for  $\cos$  and  $\sin$ , respectively.

The coordinates of four vertices of rectangle  $i$  are

$$(x_{A_{i1}}, y_{A_{i1}}) = (x_i + \frac{b_i}{2}c\phi_i - \frac{a_i}{2}s\phi_i, y_i + \frac{b_i}{2}s\phi_i + \frac{a_i}{2}c\phi_i) \quad (1)$$

$$(x_{A_{i2}}, y_{A_{i2}}) = (x_i + \frac{b_i}{2}c\phi_i + \frac{a_i}{2}s\phi_i, y_i + \frac{b_i}{2}s\phi_i - \frac{a_i}{2}c\phi_i) \quad (2)$$

$$(x_{A_{i3}}, y_{A_{i3}}) = (x_i - \frac{b_i}{2}c\phi_i + \frac{a_i}{2}s\phi_i, y_i - \frac{b_i}{2}s\phi_i - \frac{a_i}{2}c\phi_i) \quad (3)$$

$$(x_{A_{i4}}, y_{A_{i4}}) = (x_i - \frac{b_i}{2}c\phi_i - \frac{a_i}{2}s\phi_i, y_i - \frac{b_i}{2}s\phi_i + \frac{a_i}{2}c\phi_i) \quad (4)$$

Let  $\phi_{ji} = \phi_j - \phi_i$ ,  $x_{ji} = x_j - x_i$ , and  $y_{ji} = y_j - y_i$ . The distance  $d_{ij}$  between the two rectangles  $i$  and  $j$  is defined by the smallest distance from one vertex of one rectangle to the other rectangle. So, in the following, the distance from one vertex to one agent is derived.

Denote

$$p_i = \begin{bmatrix} x_i \\ y_i \end{bmatrix}, \quad (5)$$

$$p_{ij} = p_i - p_j. \quad (6)$$

Similarly,

$$p_{A_{ik}} = \begin{bmatrix} x_{A_{ik}} \\ y_{A_{ik}} \end{bmatrix} \quad (7)$$

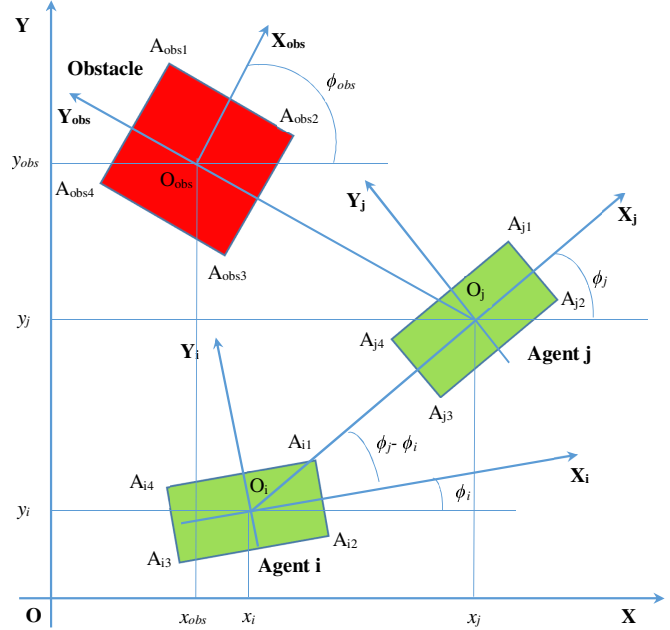


Fig. 3. Two rectangular agents and obstacle with their coordinates in the frame  $OXY$ .

for  $k = 1, \dots, 4$ . The coordinate of a vertex  $A_{jk}$  in the frame  $O_i X_i Y_i$  for  $k = 1, \dots, 4$  is

$$p_{A_{jk}}^i = R(\phi_i)(p_{A_{jk}} - p_i) \quad (8)$$

where

$$R(\cdot) = \begin{bmatrix} c(\cdot) & s(\cdot) \\ -s(\cdot) & c(\cdot) \end{bmatrix}, \quad (9)$$

and

$$p_{A_{jk}}^i = \begin{bmatrix} x_{A_{jk}}^i \\ y_{A_{jk}}^i \end{bmatrix}. \quad (10)$$

Let

$$f_{xi}(p_{A_{jk}}) = \begin{cases} |x_{A_{jk}}^i| - \frac{b_i}{2} & \text{if } |x_{A_{jk}}^i| > \frac{b_i}{2} \\ 0 & \text{otherwise,} \end{cases} \quad (11)$$

and

$$f_{yi}(p_{A_{jk}}) = \begin{cases} |y_{A_{jk}}^i| - \frac{a_i}{2} & \text{if } |y_{A_{jk}}^i| > \frac{a_i}{2} \\ 0 & \text{otherwise.} \end{cases} \quad (12)$$

The distance from  $A_{jk}$  to rectangle  $i$  is given as

$$\xi_i(p_{A_{jk}}) = \sqrt{f_{xi}(p_{A_{jk}})^2 + f_{yi}(p_{A_{jk}})^2}. \quad (13)$$

Hence, the distance between two rectangular agents  $i$  and  $j$  is defined as

$$d_{ij} = \min(\min_k(\xi_i(p_{A_{jk}})), \min_k(\xi_j(p_{A_{ik}}))) \text{ for } k = 1, \dots, 4. \quad (14)$$

It can be seen that  $d_{ij}$  is a nonsmooth function of  $p_{ij}$ ,  $\phi_{ij}$ , and  $\phi_i$ . The distance function  $d_{ij}$  possesses the following property.

*Lemma 1:*  $d_{ij}(p_{ij}, \phi_{ij}, \phi_i)$  is invariant with respect to a change of coordinates. In other words,

$$d_{ij}(p_{ij}, \phi_{ij}, \phi_i) = d_{ij}(\bar{p}_{ij}, \bar{\phi}_{ij}, \bar{\phi}_i) \quad (15)$$

where a change of coordinates is given by

$$\begin{aligned} \bar{p}_i &= R(\phi_d)(p_i - p_d) \\ \bar{\phi}_i &= \phi_i - \phi_d, \end{aligned} \quad (16)$$

where  $p_d$  is the new origin and  $\phi_d$  is the angle difference between the new and old coordinate frames,  $R(\cdot)$  is given in (9).

**Proof:** It is straightforward to verify (15) in the calculation of (14). ■

### B. Obstacle models

An obstacle can be modeled as a rectangle or circle. The distance  $\hat{d}_{ij}$  from a rectangular agent to a rectangular obstacle can be defined as that between two agents as in (14).

The distance from agent  $i$  to circular obstacle  $O_{obsj}$  with radius  $R_{obsj}$  is given as

$$\hat{d}_{ij} = \xi_i(O_{obsj}) - R_{obsj} \quad (17)$$

where  $\xi(\cdot)$  is given in (13). Note that  $\hat{d}_{ij}$  in (17) is a function of  $p_{ij}$  and  $\phi_i$ .

## III. PROBLEM STATEMENT

In this section, we present the dynamics of each agent, followed by the statement of the control objective.

### A. Agent dynamics

For the sake of simplicity, we assume that each agent has the following dynamics:

$$\dot{q}_i = u_i, \quad (18)$$

for all  $i \in N$ , where  $N$  is the set of all agents in the group. Denote  $u_i = [u_{xi}, u_{yi}, u_{\phi i}]^T$  as the control input and  $q_i = [x_i, y_i, \phi_i]^T$  as the position and orientation of agent  $i$ .

*Remark 1:* For agents with more complicated dynamics, for instance nonholonomic dynamics, backstepping techniques [42] can be employed to combine with collision/obstacle avoidance parts, which will be investigated in future work.

### B. Formation control objective

We address a formation control problem for multiple rectangular agents, and the system model and control objective are as follows.

1) *System Model:* Similar to [18], the following assumptions about the system model are made.

(a) The formation trajectory of agent  $i$  is

$$q_{if}(s_{if}) = [x_{if}(s_{if}), y_{if}(s_{if}), \phi_{if}(s_{if})]^T \quad (19)$$

where  $s_{if}$  is a parameter. The reference trajectory of agent  $i$  for a formation is denoted as

$$q_{id}(t) = [x_{id}(t), y_{id}(t), \phi_{id}(t)]^T. \quad (20)$$

The distance  $d_{ijd}$  between trajectories of agents  $i$  and  $j$  satisfies the following condition:

$$d_{ijd} \geq \delta_{ijd}, \quad (21)$$

where  $\delta_{ijd}$  is a positive constant. Note that  $d_{ijd}$  is given as in the previous section, in which  $q_i$  and  $q_j$  are substituted by  $q_{id}$  and  $q_{jd}$ , respectively. Furthermore,  $\|\dot{q}_{id}\|$  is bounded, and  $\|q_{id} - q_{jd}\|$  is bounded for bounded  $\|q_{id}\|$  and  $\|q_{jd}\|$ . Note that  $q_{id}(t)$  may not be continuous with respect to  $t$ .

(b) Agents  $i$  and  $j$  possess circular communication areas whose centers are at  $O_i$  and  $O_j$  with radii  $R_i$  and  $R_j$  (see Fig. 1). These radii satisfy the following condition:

$$\min(R_i^2, R_j^2) \geq \delta_{ijR} + \frac{a_i^2 + b_i^2}{4} + \frac{a_j^2 + b_j^2}{4}, \quad (22)$$

where  $\delta_{ijR}$  is a positive constant for all  $(i, j) \in N$  and  $j \neq i$ .

(c) Agent  $i$  broadcasts  $q_i$  and  $q_{id}$  in its communication area and receive  $q_j$  and  $q_{jd}$  broadcasting by other agents  $j$ ,  $j \in N$ ,  $j \neq i$  in the group if the points  $O_j$  are within the communication range of agent  $i$ .

(d) At the initial time  $t_0 \geq 0$ , all the agents are kept away far enough from each other, i.e.

$$d_{ij}(t_0) \geq \delta_{ij0}, \quad (23)$$

where  $\delta_{ij0}$  is a positive constant, and  $d_{ij}(t_0)$  is the distance between two agents  $i$  and  $j$ , which is derived in the previous section, evaluated at  $t = t_0$ .

2) *Control Objective:* Based on the system model above, for each agent  $i$ , design a control law  $u_i$  such that  $q_i$  tracks  $q_{id}$  while avoiding collisions with obstacles and all other agents in the group. Similar to [18],  $u_i$  is designed such that

$$\lim_{t \rightarrow \infty} (q_i(t) - q_{id}(t))(t) = 0, \quad d_{ij}(t) \geq \delta_{ij} \quad (24)$$

for all  $(i, j) \in N$ ,  $i \neq j$ , and  $t \geq t_0 \geq 0$ , where  $\delta_{ij}$  is a positive constant.

*Remark 2:* In order to avoid any possible collision with obstacles, each agent should be capable of detecting obstacles by its onboard sensors (e.g., laser range scanners or sonar sensors). Once the agent has sensed the obstacles within its sensing range, a repulsive force is applied to push it away from them (see the obstacle avoidance function  $\theta$  in the next section.)

#### IV. FORMATION CONTROL DESIGN

##### A. Potential function

A potential function is composed of a goal function  $\gamma$ , a collision avoidance function  $\beta$  and an obstacle avoidance function  $\theta$

$$\varphi = \gamma + \beta + \theta. \quad (25)$$

The goal function is designed as follows

$$\gamma = \sum_{i=1}^N \gamma_i \quad (26)$$

where

$$\gamma_i = \frac{k_1}{2}((x_i - x_{id})^2 + (y_i - y_{id})^2) + \frac{k_2}{2}(\phi_i - \phi_{id})^2 \quad (27)$$

with positive constants  $k_1, k_2$ .

*Remark 3:* We employ a similar approach as in [18]. However, our problem is more general in the sense that an obstacle avoidance function is considered.

Similar to [18],  $p$ -times differentiable step functions are employed to construct the collision avoidance and obstacle avoidance functions, which play a key role in the control design. A  $p$ -time differentiable step function  $h(x, a, b)$  posses the following properties [18]:

- 1)  $h(x, a, b) = 0$ , for  $-\infty < x \leq a$ .
- 2)  $h(x, a, b) = 1$ , for  $b \leq x < \infty$ .
- 3)  $0 < h(x, a, b) < 1$ , for  $a < x < b$ .
- 4)  $h(x, a, b)$  is  $p$ -times differentiable.

The collision avoidance function is designed as

$$\beta = \sum_{i=1}^{N-1} \sum_{j=i+1}^N \beta_{ij} \quad (28)$$

where  $\beta_{ij}$  is a function of  $d_{ij}$ , and it is designed as

$$\beta_{ij} = k_{ij} \frac{1 - h_{ij}(\Delta_{ij}, a_{ij}, b_{ij})}{\Delta_{ij}} \quad (29)$$

where  $k_{ij}$  is a positive parameter,  $\Delta_{ij} = d_{ij}^2$  and  $h_{ij}(\Delta_{ij}, a_{ij}, b_{ij})$  is a  $p$ -times differentiable smooth step function. A choice of  $h_{ij}$  can be taken as in [18], [43]. The constant  $a_{ij}$  and  $b_{ij}$  are chosen such that

$$0 < a_{ij} < b_{ij} \leq \min(\delta_{ijd}, \delta_{ijR}) - \mu_{ij} = \tau_{ijd}, \quad (30)$$

where  $\delta_{ijd}, \delta_{ijR}$  are given in (21) and (22), and  $\mu_{ij}$  is a positive constant.

The obstacle avoidance function is designed as follows:

$$\theta = \sum_{i=1}^N \sum_{k=1}^M \theta_{ik} \quad (31)$$

where  $M$  is number of obstacles,  $\theta_{ik}$  is a function of  $\hat{d}_{ik}$ , which is the distance from agent  $i$  to obstacle  $k$  and it is designed as

$$\theta_{ik} = \hat{k}_{ik} \frac{1 - \hat{h}_{ik}(\hat{\Delta}_{ik}, \hat{a}_{ik}, \hat{b}_{ik})}{\hat{\Delta}_{ik}} \quad (32)$$

where  $\hat{k}_{ik}$  is a positive parameter,  $\hat{\Delta}_{ik} = \hat{d}_{ik}^2$  and  $\hat{h}_{ik}(\hat{\Delta}_{ik}, \hat{a}_{ik}, \hat{b}_{ik})$  is a  $p$ -times differentiable smooth step function. A choice of  $\hat{h}_{ik}$  can be taken as in [18]. The constant  $\hat{a}_{ik}$  and  $\hat{b}_{ik}$  are chosen such that

$$0 < \hat{a}_{ik} < \hat{b}_{ik} \leq \tau_{iko}^2, \quad (33)$$

where

$$\tau_{iko} = \nu_i - \frac{\sqrt{a_i^2 + b_i^2}}{2} - \mu_{ik} > 0, \quad (34)$$

with  $\nu_i$  being the sensing range of agent  $i$  and  $\mu_{ik}$  being a positive constant.

*Remark 4:* From the definition of  $\beta_{ij}$  and the properties of the step function  $h_{ij}(\Delta_{ij}, a_{ij}, b_{ij})$ , we observe that when  $\delta_{ij} \geq \sqrt{b_{ij}}$ ,  $\beta_{ij} = 0$ . When the distance between agents  $i$  and  $j$  is close enough, i.e.  $\delta_{ij} < \sqrt{b_{ij}}$ ,  $\beta_{ij} > 0$ . This means the collision avoidance between agents  $i$  and  $j$  is active. Similarly,  $\theta_{ik} = 0$ , when  $\hat{\delta}_{ik} \geq \sqrt{b_{ik}}$ . When the distance between agent  $i$  and obstacle  $k$  is close enough, i.e.  $\hat{\delta}_{ik} < \sqrt{b_{ik}}$ ,  $\theta_{ik} > 0$ . This implies the obstacle avoidance for agent  $i$  is active.

##### B. Control design

Let us define  $p_{id} = [x_{id}, y_{id}]^T$ , and  $p_{ijd} = p_{id} - p_{jd}$  for all  $(i, j) \in N$  and  $j \neq i$ . Substituting (27), (28), and (31) into (25), we obtain

$$\begin{aligned} \varphi = & \frac{k_1}{2} \sum_{i=1}^N \|p_i - p_{id}\|^2 + \frac{k_2}{2} \sum_{i=1}^N k_2 (\phi_i - \phi_{id})^2 \\ & + \sum_{i=1}^{N-1} \sum_{j=i+1}^N \beta_{ij} + \sum_{i=1}^N \sum_{k=1}^M \theta_{ik}. \end{aligned} \quad (35)$$

Differentiating both sides of (35), we obtain the following differential inclusion

$$\begin{aligned} \dot{\varphi} \in & \sum_{i=1}^N \left[ k_1 (p_i - p_{id}) + D_i^\beta + D_i^\theta \right]^T (\dot{p}_i - \dot{p}_{id}) \\ & + \sum_{i=1}^N \left[ k_2 (\phi_i - \phi_{id}) + E_i^\beta + E_i^\theta \right] (\dot{\phi}_i - \dot{\phi}_{id}) \\ & + (D_i^\beta + D_i^\theta)^T \dot{p}_{id} + (E_i^\beta + E_i^\theta) \dot{\phi}_{id}, \end{aligned} \quad (36)$$

where

$$D_i^\beta = - \sum_{j=1}^{i-1} \beta'_{ji} G_{ji}^\beta + \sum_{j=i+1}^N \beta'_{ij} G_{ij}^\beta, \quad (37)$$

$$E_i^\beta = - \sum_{j=1}^{i-1} \beta'_{ji} H_{ji}^\beta + \sum_{j=i+1}^N (\beta'_{ij} (H_{ij}^\beta + L_{ij}^\beta)), \quad (38)$$

$$D_i^\theta = \sum_{k=1}^M \theta'_{ik} G_{ik}^\theta, \quad (39)$$

$$E_i^\theta = \sum_{k=1}^M (\theta'_{ik} (H_{ik}^\theta + L_{ik}^\theta)), \quad (40)$$

$$G_{ij}^\beta = \frac{\partial \Delta_{ij}}{\partial p_{ij}} (R(\phi_{id})p_{ij}, \phi_{ij}, \phi_i - \phi_{id}), \quad (41)$$

$$H_{ij}^\beta = \frac{\partial \Delta_{ij}}{\partial \phi_{ij}} (R(\phi_{id})p_{ij}, \phi_{ij}, \phi_i - \phi_{id}), \quad (42)$$

$$L_{ij}^\beta = \frac{\partial \Delta_{ij}}{\partial \phi_i} (R(\phi_{id})p_{ij}, \phi_{ij}, \phi_i - \phi_{id}), \quad (43)$$

$$G_{ik}^\theta = \frac{\partial \hat{\Delta}_{ik}}{\partial p_{ik}} (R(\phi_{id})p_{ik}, \phi_{ik}, \phi_i - \phi_{id}), \quad (44)$$

$$H_{ik}^\theta = \frac{\partial \hat{\Delta}_{ik}}{\partial \phi_{ik}} (R(\phi_{id})p_{ik}, \phi_{ik}, \phi_i - \phi_{id}), \quad (45)$$

$$L_{ik}^\theta = \frac{\partial \hat{\Delta}_{ik}}{\partial \phi_i} (R(\phi_{id})p_{ik}, \phi_{ik}, \phi_i - \phi_{id}), \quad (46)$$

and

$$\beta'_{ij} = \frac{\partial \beta_{ij}}{\partial \Delta_{ij}}, \theta'_{ik} = \frac{\partial \theta_{ik}}{\partial \hat{\Delta}_{ik}}. \quad (47)$$

Let

$$\begin{aligned} \Omega_{pi} &= k_1(p_i - p_{id}) + D_i^\beta + D_i^\theta, \\ \Omega_{\phi i} &= k_2(\phi_i - \phi_{id}) + E_i^\beta + E_i^\theta. \end{aligned} \quad (48)$$

From (36), we choose a control law for agent  $i$  as follows

$$\begin{aligned} \begin{bmatrix} u_{xi} \\ u_{yi} \end{bmatrix} &= \rho_i(-c_1 \Omega_{pi} + \dot{p}_{id}), \\ u_{\phi i} &= \rho_i(-c_2 \Omega_{\phi i} + \dot{\phi}_{id}), \end{aligned} \quad (49)$$

where  $c_1$  and  $c_2$  are positive constants,  $\rho_i$  is a parameter, which is 0 or 1. The parameter  $\rho_i$  determines whether agent  $i$  proceeds to carry out its objective or stand stills depending on the collision avoidance algorithm. Assume agent  $i$  has higher priority than agent  $j$ . When collision avoidance between agents  $i$  and  $j$  is active,  $\rho_i = 1$  and  $\rho_j = 0$ .

As explained in Remark 4, the collision avoidance between agents  $i$  and  $j$  is active when  $\delta_{ij} < \sqrt{b_{ij}}$ . Similarly, the obstacle avoidance between agent  $i$  and obstacle  $k$  is active when  $\hat{\delta}_{ik} < \sqrt{\hat{b}_{ik}}$ . When collision and/or obstacle avoidance is active, i.e.  $\beta_{ij} \neq 0$  and  $\theta_{ik} \neq 0$ , we can choose a reference trajectory for agent  $i$  such that  $\dot{q}_{id} = [\dot{p}_{id}^T, \dot{\phi}_{id}^T]^T = 0$ .

When no collision and obstacle avoidance is active,  $\delta_{ij} \geq \sqrt{b_{ij}}$  for all  $j$ , and  $\hat{\delta}_{ik} \geq \sqrt{\hat{b}_{ik}}$  for all  $k$ . In this case,  $\beta_{ij} = 0$  and  $\theta_{ik} = 0$ . Hence, from (37), (38), (39), and (40),

$$D_i^\beta = D_i^\theta = 0, \quad (50)$$

$$E_i^\beta = E_i^\theta = 0. \quad (51)$$

With the above strategy of choosing a reference trajectory for agent  $i$ , it follows that

$$(D_i^\beta + D_i^\theta)^T \dot{p}_{id} + (E_i^\beta + E_i^\theta) \dot{\phi}_{id} = 0. \quad (52)$$

We denote such a reference trajectory as  $q_{ie}$ , which will be designed later. When no collision/obstacle avoidance is active,  $q_{id} = q_{if}$  where  $q_{if}$  is the formation reference of agent  $i$ .

### C. Stability Analysis

*Remark 5:* Note that  $d_{ij}$  and  $\hat{d}_{ik}$  are not smooth, so are  $\Delta_{ij}$  and  $\hat{\Delta}_{ik}$ . Hence, (41), (42), (43), (44), (45), and (46) are not continuous. Therefore, neither is the control law (49), which makes the closed-loop system become a differential inclusion. To study the behavior of the closed-loop system, we need to employ the LaSalle's invariance principle for switched nonlinear systems [44].

The guarantee of collision avoidance among rectangular agents and the convergence of formation performance are presented in the following theorem.

*Theorem 1:* Under System Model III-B1, the closed-loop system under the control input vector given in (49) for agent  $i$  satisfies the following results:

- 1) There are no collisions between any agents and obstacle avoidance is guaranteed. In addition, the closed-loop system is forward complete.
- 2) The velocity of each agent satisfies

$$\begin{aligned} \lim_{t \rightarrow \infty} (\dot{x}_i - \dot{x}_{id}) &= 0 \\ \lim_{t \rightarrow \infty} (\dot{y}_i - \dot{y}_{id}) &= 0 \\ \lim_{t \rightarrow \infty} (\dot{\phi}_i - \dot{\phi}_{id}) &= 0. \end{aligned} \quad (53)$$

**Proof:** Under the control law (49), the closed-loop system of (18) is given as

$$\begin{aligned} \begin{bmatrix} \dot{x}_i \\ \dot{y}_i \end{bmatrix} &\in \rho_i(-c_1 \Omega_{pi} + \dot{p}_{id}), \\ \dot{\phi}_i &\in \rho_i(-c_2 \Omega_{\phi i} + \dot{\phi}_{id}), \end{aligned} \quad (54)$$

and the derivative of  $\varphi$  is given as

$$\dot{\varphi} \in -c_1 \sum_{i=1}^N \rho_i \Omega_{pi}^T \Omega_{pi} - c_2 \sum_{i=1}^N \rho_i \Omega_{\phi i}^T \Omega_{\phi i}. \quad (55)$$

Equation (55) shows that  $\dot{\varphi} \leq 0$ . Hence, according to the extended LaSalle's Invariance Principle for switched nonlinear systems [44],  $\varphi$  is bounded for  $t \geq t_0 \geq 0$  and the state variables converge asymptotically to the set where  $\dot{\varphi} = 0$ . Since  $\varphi$  is bounded,  $\beta_{ij}$  and  $\theta_{ik}$  are bounded. This implies  $d_{ij} > 0$  and  $\hat{d}_{ik} > 0$ . Hence, no collision takes place between any two agents and obstacle avoidance is satisfied. Note that during the evolution of agent  $i$  to avoid collision/obstacle avoidance,  $d_{ij}(t)$  may not satisfy the control objective in (24). Once all obstacle/collision avoidance is fulfilled, agent  $i$  continues to track its reference trajectory  $q_{id}$ . Furthermore, the boundedness of  $\varphi$  for  $t \geq t_0 \geq 0$  implies the boundedness of  $(p_i - p_{id})$  and  $(\phi_i - \phi_{id})$ . In other words, or  $(q_i - q_{id})$  is bounded for  $t \geq t_0 \geq 0$ . Hence, the closed-loop system is forward complete.

From (55), we find the set where  $\dot{\varphi} = 0$ . Here, we consider the following equation

$$c_1 \sum_{i=1}^N \rho_i \Omega_{pi}^T \Omega_{pi} - c_2 \sum_{i=1}^N \rho_i \Omega_{\phi i}^T \Omega_{\phi i} = 0. \quad (56)$$

When  $\rho_i = 0$ , the collision avoidance is active for agent  $i$ . Hence,  $q_{id} = 0$  as presented in the control design procedure in Section IV-B. As a result,

$$\dot{x}_i = \dot{x}_{id} = 0, \quad (57)$$

$$\dot{y}_i = \dot{y}_{id} = 0, \quad (58)$$

$$\dot{\phi}_i = \dot{\phi}_{id} = 0. \quad (59)$$

For agent  $i$  with  $\rho_i = 1$ , (56) implies that  $\Omega_{pi} = 0$  and  $\Omega_{\phi i} = 0$ . Using these values in (54), we obtain the expressions as in (53). ■

*Remark 6:* The reference trajectory  $q_{id}$  is designed to help agent  $i$  get through collision/obstacle avoidance scenarios. After that, no collision/obstacle avoidance is active. Thus,  $\rho_i = 1$ ,  $D_i^\beta = D_i^\theta = 0$ , and  $E_i^\beta = E_i^\theta = 0$ . From (48) and (49),

$$\begin{aligned} \begin{bmatrix} u_{xi} \\ u_{yi} \end{bmatrix} &= -c_1 k_1 \begin{bmatrix} x_i - x_{id} \\ y_i - y_{id} \end{bmatrix} + \dot{p}_{id}, \\ u_{\phi i} &= -c_2 k_2 (\phi_i - \phi_{id}) + \dot{\phi}_{id}. \end{aligned} \quad (60)$$

Using (60) in the original dynamics of agent  $i$  in (18) yields

$$\begin{aligned} \dot{x}_i &= -c_1 k_1 (x_i - x_{id}) + \dot{x}_{id} \\ \dot{y}_i &= -c_1 k_1 (y_i - y_{id}) + \dot{y}_{id} \\ \dot{\phi}_i &= -c_2 k_2 (\phi_i - \phi_{id}) + \dot{\phi}_{id}. \end{aligned} \quad (61)$$

This implies  $q_i$  converges to  $q_{id}$  as  $t \rightarrow \infty$ .

#### D. Reference trajectory design for collision/obstacle avoidance

Assume  $q_{if}$  is designed as the formation reference of agent  $i$ . When obstacle/collision avoidance is active, a reference trajectory  $q_{id}$  is defined for agent  $i$  to pass possible obstacles. During this phase,  $\dot{q}_{id} = 0$ . For each rectangular obstacle, there are 4 escape references associated with 4 vertexes of the obstacle.

Denote  $V_{A_{jk}}^i$  be an escape reference associated with  $A_{jk}$  of agent  $j$  for agent  $i$ . The coordinates of  $V_{A_{jk}}^i$  are given as follows

$$\begin{aligned} p_{V_{A_{j1}}^i}^T &= (x_j + (\frac{b_j}{2} + \alpha_i)c\phi_j - (\frac{a_j}{2} + \alpha_i)s\phi_j, y_j \\ &\quad + (\frac{b_j}{2} + \alpha_i)s\phi_j + (\frac{a_j}{2} + \alpha_i)c\phi_j) \end{aligned} \quad (62)$$

$$\begin{aligned} p_{V_{A_{j2}}^i}^T &= (x_j + (\frac{b_j}{2} + \alpha_i)c\phi_j + (\frac{a_j}{2} + \alpha_i)s\phi_j, y_j \\ &\quad + (\frac{b_j}{2} + \alpha_i)s\phi_j - (\frac{a_j}{2} + \alpha_i)c\phi_j) \end{aligned} \quad (63)$$

$$\begin{aligned} p_{V_{A_{j3}}^i}^T &= (x_j - (\frac{b_j}{2} + \alpha_i)c\phi_j + (\frac{a_j}{2} + \alpha_i)s\phi_j, y_j \\ &\quad - (\frac{b_j}{2} + \alpha_i)s\phi_j - (\frac{a_j}{2} + \alpha_i)c\phi_j) \end{aligned} \quad (64)$$

$$\begin{aligned} p_{V_{A_{j4}}^i}^T &= (x_j - (\frac{b_j}{2} + \alpha_i)c\phi_j - (\frac{a_j}{2} + \alpha_i)s\phi_j, y_j \\ &\quad - (\frac{b_j}{2} + \alpha_i)s\phi_j + (\frac{a_j}{2} + \alpha_i)c\phi_j) \end{aligned} \quad (65)$$

where

$$\alpha_i = \frac{\sqrt{b_i^2 + a_i^2}}{2} + \eta_i \quad (66)$$

with  $\eta_i > 0$  being a safety parameter. The heading angle reference  $\phi_{id} = \phi_{if}(t_{ij})$  where  $t_{ij}$  is the time when the collision avoidance is activated.

Denote  $V_{A_{obk}}^i$  be an escape reference associated with  $A_{obk}$  of obstacle  $k$  for agent  $i$ . Its coordinates are similar to the above case.

When an obstacle is a circle, an escape reference can be determined as follows. Let  $r_{obj}$  be the radius of obstacle  $A_{obj}$  whose center lies at  $p_{A_{obj}}$ . Let

$$p_e = R(\phi_{obj}) \begin{bmatrix} x_{A_{obj}} - x_i \\ y_{A_{obj}} - y_i \end{bmatrix} \quad (67)$$

where  $R(\cdot)$  is given in (9),

$$\phi_{obj} = -\frac{\pi}{2} + \text{atan}\left(\frac{y_{if} - y_i}{x_{if} - x_i}\right). \quad (68)$$

and  $(x_{if}, y_{if})$  is the coordinate of the destination of agent  $i$ .

If  $p_e(1) > 0$ ,

$$p_{V_{A_{obj}}^i} = R^T(\phi_{obj}) \begin{bmatrix} p_e(1) - r_{ei} \\ p_e(2) \end{bmatrix} + \begin{bmatrix} x_i \\ y_i \end{bmatrix} \quad (69)$$

else

$$p_{V_{A_{obj}}^i} = R^T(\phi_{obj}) \begin{bmatrix} p_e(1) + r_{ei} \\ p_e(2) \end{bmatrix} + \begin{bmatrix} x_i \\ y_i \end{bmatrix} \quad (70)$$

where

$$r_{ei} = r_{obj} + \frac{\sqrt{a_i^2 + b_i^2}}{2} + \eta_i. \quad (71)$$

Denote  $\sigma_{ij}$  as the orientation of agent  $i$  with respect to agent  $j$ . This variable is employed to determine which direction agent  $i$  should follow to avoid possible collisions with other agents. Initially,  $\sigma_{ij} = 0$ . If the agent  $i$  moves counterclockwise,  $\sigma_{ij} = 1$ . If it moves clockwise,  $\sigma_{ij} = -1$ . Let  $I_{ij}$  be an engagement index of agent  $i$  and agent  $j$  when collision avoidance is active. When  $I_{ij} = 1$ , one agent with less priority will stand still and act as an obstacle.

Similarly, denote  $\hat{\sigma}_{ik}$  as the orientation of agent  $i$  with respect to obstacle  $k$ . If the agent  $i$  moves counterclockwise,  $\hat{\sigma}_{ik} = 1$ . If it moves clockwise,  $\hat{\sigma}_{ik} = -1$ . Let  $\hat{I}_{ik}$  be an engagement index of agent  $i$  and obstacle  $k$  when collision avoidance is active.

Let  $d(O_i, O_j)$  be the distance between two objects  $i$  and  $j$ . Let  $q_{if}$  be the formation reference of agent  $i$ . Our purpose is to design  $q_{id}$  such that agent  $i$  avoid any possible collision and eventually track its formation reference.

We have the algorithm of collision avoidance among agents as summarized in Algorithm 1. The algorithm for obstacle avoidance is similar to Algorithm 1 where a rectangular obstacle plays the role of a rectangular agent. Circular obstacle avoidance is carried out by using the escape reference in (69) and (70).

---

**Algorithm 1** Collision Avoidance Algorithm
 

---

```

set  $\sigma_{ij} = 0, I_{ij} = 0$  for  $i = 1, \dots, N$ , and  $j = 2, \dots, N$  ( $i \neq j$ ).
1: for each iteration  $t = t_l$  do
2:   for each agent  $i$  do
3:     for each agent  $j$  ( $i \neq j$ ) do
4:       if  $d(O_i, O_j) < \mu_{ij}$  where  $\mu_{ij} \geq b_{ij}$  is a safety
         distance then
5:         if  $I_{ij} = 0$  then record the time  $t_{ij}$ 
6:         end if
7:         set  $I_{ij} = 1$ 
8:       end if
9:     end for
10:   end for
11:   Let  $t_e = \max t_{ij}$ . Define a coordinate transfor-
     mation  $p^e = R(\phi_e)(p - p_i(t_e))$  where  $\phi_e = -\frac{\pi}{2} +$ 
      $\text{atan}(\frac{y_{if} - y_i(t_e)}{x_{if} - x_i(t_e)})$  with  $(x_{if}, y_{if})$  being the coordinate of
     the formation reference of agent  $i$ .
12:   Let  $P(i) \in \mathbb{N}$  be a priority function of agent  $i$ , which
     satisfies  $P(i) \neq P(j)$  if  $i \neq j$ .
13:   for each agent  $j$  ( $i \neq j$ ) do
14:     if  $I_{ij} = 1$  then
15:       if  $P(i) < P(j)$  then  $\rho_i = 0$ 
16:       else  $\rho_i = 1$ 
17:       end if
18:       if  $\sigma_{ij} = 0$  then  $\Lambda = \max_v x_{A_{jv}}^e + \min x_{A_{jv}}^e$ 
19:       if  $\Lambda \geq 0$  then set  $\sigma_{ij} = -1$ 
20:       else set  $\sigma_{ij} = 1$ 
21:       end if
22:     end if
23:   end for
24:   end for
25:   if  $\sigma_{ij} \neq 0$  then
26:     if  $|q_{id} - q_i(t_l)| < \epsilon$  where  $\epsilon$  is a small positive
         number then set  $t_e = t_l$ 
27:     end if
28:   end if
29:   for each agent  $j$  ( $i \neq j$ ) do
30:     if agent  $i$  has higher priority than agent  $j$  then
31:       if  $d(O_i O_{if}, O_j) > \tilde{\mu}_{ij}$  and  $I_{ij} = 1$  where
          $d(O_i O_{if}, O_j)$  is the distance from agent  $j$  to the line
         connecting  $O_i$  and  $O_{if}$  and  $O_{if}$  is the reference point
         whose coordinate is  $q_{if}$  then  $I_{ij} = 0$  and  $\sigma_{ij} = 0$ .
32:       end if
33:     end if
34:   end for
35:   if  $\sum I_{ij} \geq 2$  then  $\rho_i = 1$ 
36:   end if
37:   if  $\sum I_{ij} = 0$  then set  $\sigma_{ij} = 0, q_{id} = q_{if}$ .
38:   else
39:     for each agent  $j$  ( $i \neq j$ ) do
40:       Find  $\min_{j,v} (|x_{V_{A_{jv}}}^e|)$  subject to  $I_{ij} = 1,$ 
 $\sigma_{ij} x_{V_{A_{jv}}}^e > 0$ . Let the solution be  $V_{A_{min}}^i$ .
41:       Set  $p_{id} = p_{V_{A_{min}}^i}; \phi_{id} = \phi_{if}(t_e)$ .
42:     end for
43:   end if
44: end for

```

---

## V. SIMULATION RESULTS

In this section we test our proposed formation control algorithm for both free space and obstacle space. For free space we investigate typical cases of lattice and circular formation, respectively. Also for the case of obstacle space we check the proposed algorithm for typical case of straight line for obstacles with different sizes and shapes. The proposed algorithm can work for many other formation shapes such as V-shape and  $\infty$  shape, however due to the similarity and limited space we do not report here.

### A. Free Space

1) *Lattice formation*: We use 15 rectangular agents with  $a_i = 1, b_i = 3$ . An agent whose number is smaller than that of another agent has higher priority. The initial conditions are  $q_i(0) = [R_0 \sin(\frac{2\pi(i-1)}{R_0} + \pi), R_0 \cos(\frac{2\pi(i-1)}{R_0} + \pi), 2\pi + \text{rand}(\cdot)]^T$  with  $R_0 = 10$  for  $i = 1, \dots, 5$  and  $R_0 = 20$  for the other agents, and  $\text{rand}(\cdot)$  a random number between 0 and 1. The control parameters are chosen as  $C_1 = 10^4 \text{diag}(1, 1), K_1 = C_1^{-1}, c_2 = 10^4, k_2 = 1/c_2$ . The signal  $s_{if}(t)$  tracks the common trajectory reference parameter  $s_{od}(t)$  by the following differential equation:

$$\dot{s}_{if}(t) = -50(s_{if}(t) - s_{od}(t)) + \dot{s}_{od}(t). \quad (72)$$

We choose  $s_{if}(0) = 0, s_{od}(0) = 0$

We implement a lattice formation by choosing  $q_{if} = [x_{if}, R_0 \cos(\frac{4\pi(i-1)}{R_0} + \pi), 0]^T$  with  $R_0 = 10$  for  $i = 1, \dots, 5$  and  $R_0 = 20$  for the other agents. We choose  $x_{if} = s_{if} - R_0 \sin(\frac{4\pi(i-1)}{R_0} + \pi)$ . The parameters of  $\beta_{ij}$  in (29) are taken as  $a_{ij} = 0$  and  $b_{ij} = 0.5$ . The other parameters are:  $k_{ij} = 10^{-5}, \mu_{ij} = 0.8, \epsilon = 0.2$ , and  $\eta_i = 0.6$ .

Figure 4 (a) shows 15 rectangular agents forming a lattice formation. We can see that they can form a completed lattice shape after about 16 seconds. This clearly demonstrates the efficiency of the proposed control algorithm.

Denote

$$d_{ij}^* = \left( \prod_{j=1, j \neq i}^N d_{i,j} \right)^{1/(N-1)} \quad (73)$$

as the distance representative of agent  $i$ .

Figure 4 (b) shows that the distance  $d_{ij}^*$  (defined above) representatives of the rectangular agents converge to an equilibrium. The state errors of the agents, i.e.  $(x_i - x_{id}), (y_i - y_{id}), (\phi_i - \phi_{id})$ , are illustrated in Figure 4 (c, d, e).

2) *Circular formation*: In the circular formation we test for both single and multi-circle formations. In the single circle formation, we deploy 15 rectangular agents randomly. The initial conditions and other control parameters are chosen the same as the line formation case. We implement a circular formation by choosing  $q_{if} = [20 \cos(s_{id} + \frac{2\pi}{N}i), 20 \sin(s_{id} + \frac{2\pi}{N}i), \frac{\pi}{2} + s_{if} + \frac{2\pi}{N}i]^T$ . We choose  $s_{if} = 0.5t$ . The parameters of  $\beta_{ij}$  in (29) are taken as  $a_{ij} = 0$  and  $b_{ij} = 0.5$ . The other parameters are:  $k_{ij} = 10^{-5}, \mu_{ij} = 0.8, \epsilon = 0.2$ , and  $\eta_i = 0.6$ .

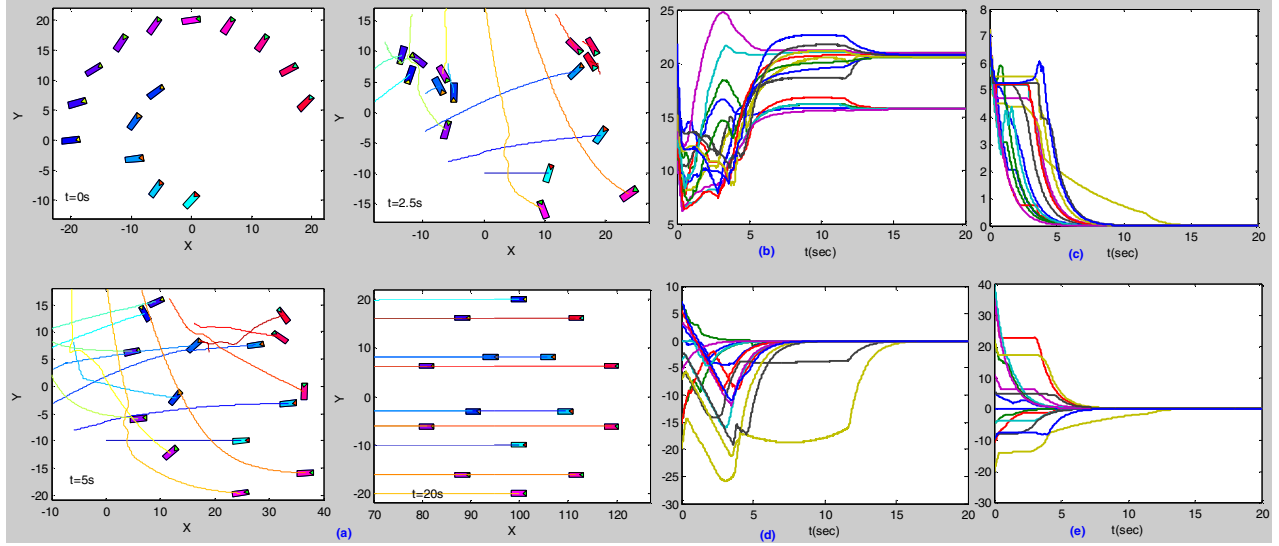


Fig. 4. (a) The snapshots of agent’s movements and the agreement of agent’s positions and orientations in “lattice” formation; (b) Distance representative  $d_{ij}^*$ ; (c) Tracking errors in the heading angles; (d) Tracking errors in the x coordinate; (e) Tracking errors in the y coordinate.

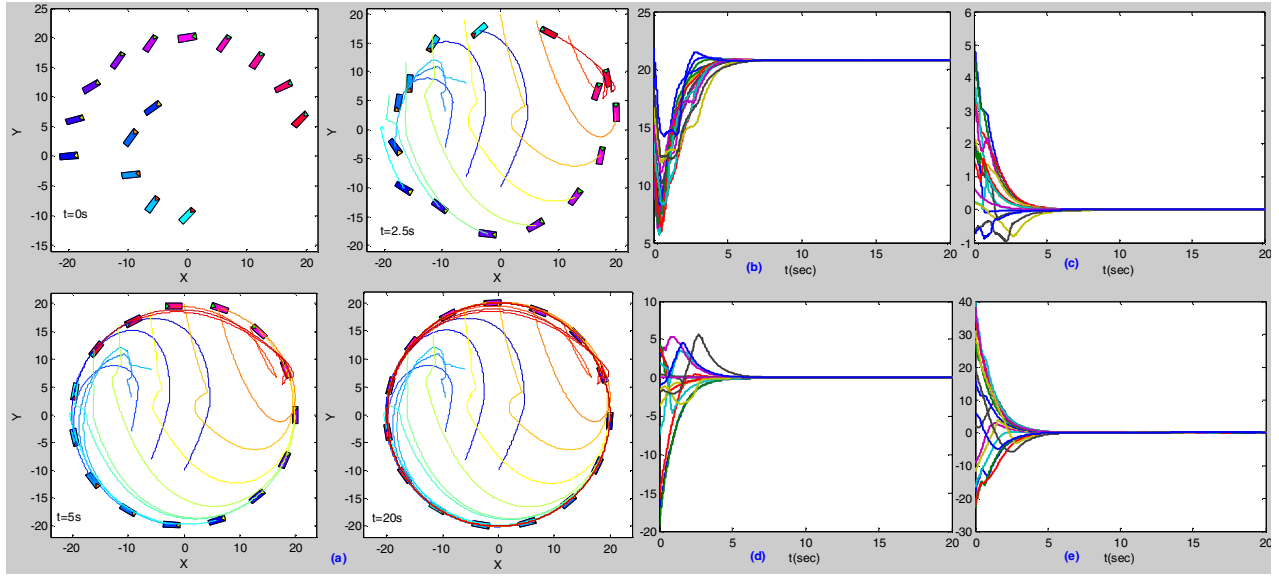


Fig. 5. (a) The snapshots of agent’s movements and the agreement of agent’s positions and orientations in “circular” formation; (b) Distance representative  $d_{ij}^*$ ; (c) Tracking errors in the heading angles; (d) Tracking errors in the x coordinate; (e) Tracking errors in the y coordinate.

For multi-circle formation, 15 rectangular agents are randomly deployed. The initial conditions and other control parameters are chosen the same as the line formation case. We implement a circular formation by choosing  $q_{if} = [(15+3(i-1)) \cos(s_{if}), (15+3(i-1)) \sin(s_{if}), \pi/2+s_{if}]^T$ . We choose  $s_{if} = 0.3t$ . The parameters of  $\beta_{ij}$  in (29) are taken as  $a_{ij} = 0$  and  $b_{ij} = 0.5$ . The parameter  $k_{ij}$  is  $10^{-5}$ . The other parameters are:  $k_{ij} = 10^{-5}$ ,  $\mu_{ij} = 0.8$ ,  $\epsilon = 0.2$ , and  $\eta_i = 0.6$ .

Figures 5 and 6 (a) show 15 rectangular agents forming single and multi-circle formation, respectively. It is seen that they form a completed circular shape after about 6 seconds. This illustrates the usefulness of our scheme.

Figures 5 and 6 (b) show that the distance  $d_{ij}^*$  (defined above) representatives of the rectangular agents converge to an equilibrium. The state errors of the agents, i.e.  $(x_i - x_{id})$ ,  $(y_i - y_{id})$ ,  $(\phi_i - \phi_{id})$ , are shown in Figures 5 and 6 (c, d, e), respectively.

### B. Obstacle Avoidance

We use 15 rectangular agents with  $a_i = 1$ ,  $b_i = 3$ . The initial conditions are  $q_i(0) = [R_0 \sin(\frac{2\pi(i-1)}{R_0} + \pi), R_0 \cos(\frac{2\pi(i-1)}{R_0} + \pi), 2\pi + \text{rand}(\cdot)]^T$  with  $R_0 = 10$  for  $i = 1, \dots, 5$  and  $R_0 = 20$  for the other agents, and  $\text{rand}(\cdot)$  a random number between 0 and 1. We used 5 different size rectangular and circle obstacles where the rectangular

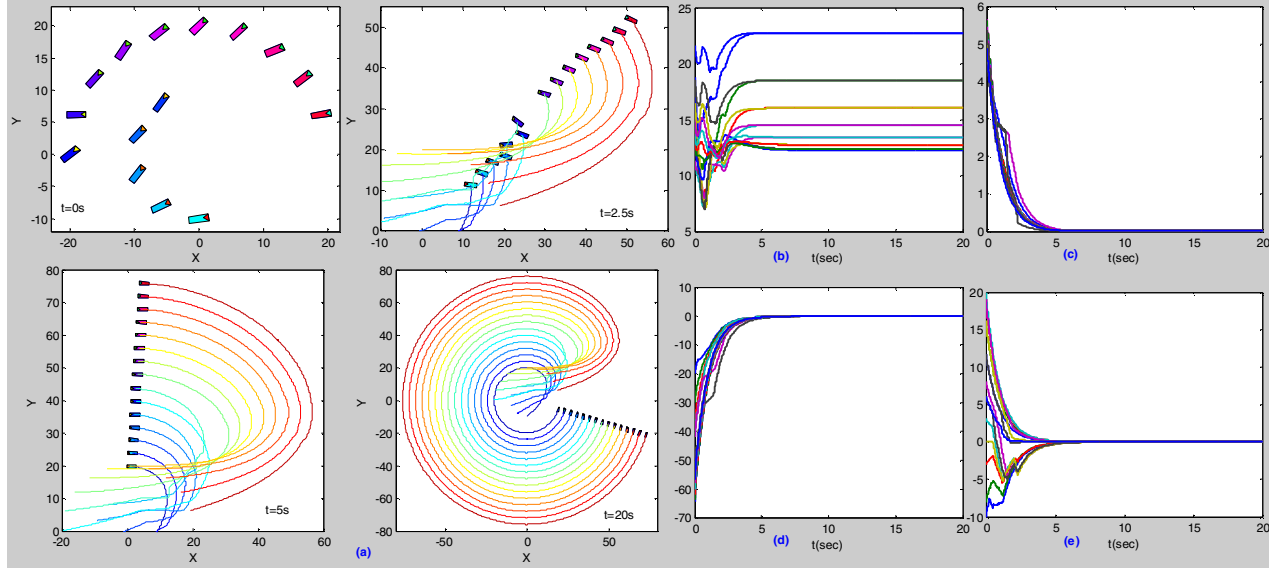


Fig. 6. (a) The snapshots of agent's movements and the agreement of agent's positions and orientations in "multi-circle" formation; (b) Distance representative  $d_{ij}^*$ ; (c) Tracking errors in the heading angles; (d) Tracking errors in the x coordinate; (e) Tracking errors in the y coordinate.

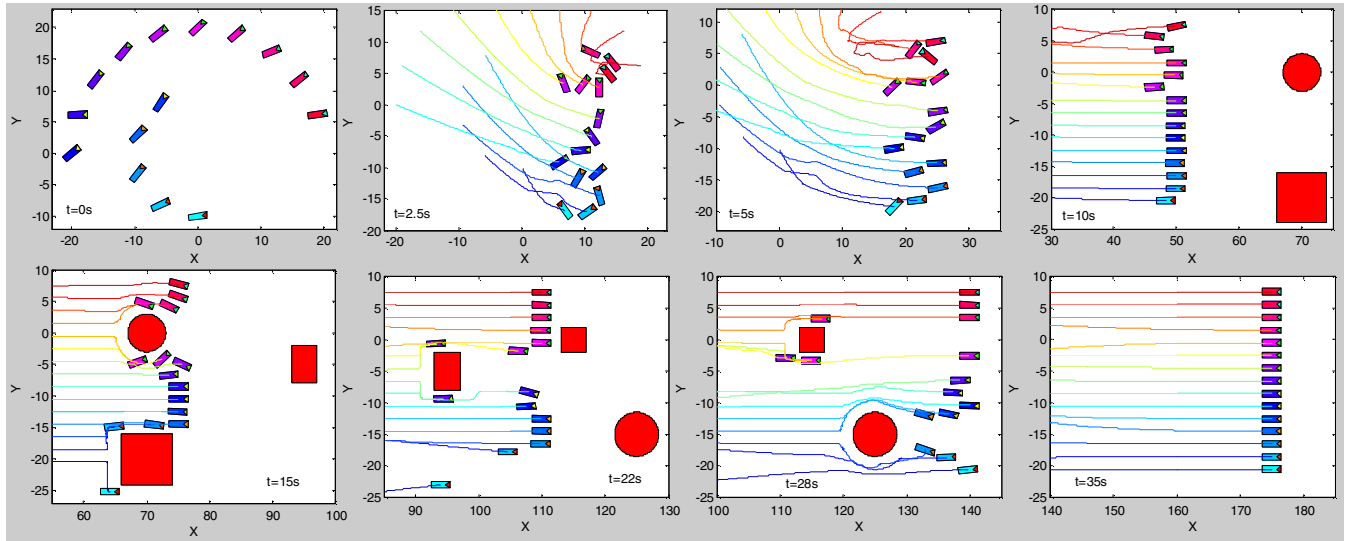


Fig. 7. The snapshots of agent's movements forming "line" formation and the agreement of agent's positions and orientations in obstacle environment.

obstacles are located at  $L_2 = \begin{bmatrix} 70 & 95 & 115 \\ -20 & -5 & 0 \\ 0 & \frac{\pi}{2} & \pi \end{bmatrix}$  while

the last row of the matrix  $L_2$  represents the orientation of the related obstacle and  $S_2 = \begin{bmatrix} 8 & 6 & 4 \\ 8 & 4 & 4 \end{bmatrix}$  shows the

size of the obstacles and  $L_3 = \begin{bmatrix} 70 & 125 \\ 0 & -15 \\ 3 & 3.5 \end{bmatrix}$  demonstrates

the circle obstacles where the last row of the matrix  $L_3$  presents the related radii. The control parameters are chosen as  $C_1 = 10^4 \text{diag}(1, 1)$ ,  $K_1 = C_1^{-1}$ ,  $c_2 = 10^4$ ,  $k_2 = 1/c_2$ . We implement a straight-line formation by choosing  $q_{if} = [s_{if}, -\frac{3N}{2} + 2i, 0]^T$  with  $s_{if}(0) = 0$ . The signal  $s_{if}(t)$  tracks the common trajectory reference parameter  $s_{od}(t)$  by the

following differential equation:

$$\dot{s}_{if}(t) = -50(s_{if}(t) - s_{od}(t)) + \dot{s}_{od}(t). \quad (74)$$

We choose  $s_{if}(0) = 0$ ,  $s_{od}(t) = 5t$ , and hence  $\dot{s}_{od} = 5$ . The parameters of  $\beta_{ij}$  in (30) are taken as  $a_{ij} = 0$  and  $b_{ij} = 0.5$ . The parameter  $k_{ij}$  of  $\beta_{ij}$  is  $10^{-5}$  and the parameters of  $\theta_{ik}$  in (33) are taken as  $\hat{a}_{ik} = 0$  and  $\hat{b}_{ik} = 0.5$ . The parameter  $\hat{k}_{ik}$  of  $\theta_{ik}$  is  $10^{-5}$ . The parameters of  $\beta_{ij}$  in (29) are taken as  $a_{ij} = 0$  and  $b_{ij} = 0.5$ . The other parameters are:  $\mu_{ij} = 0.8$ ,  $\epsilon = 0.2$ , and  $\eta_i = 0.6$ .

Figure 7 shows 15 rectangular agents forming a line-formation while avoiding the obstacles. Initially, 15 agents were randomly deployed in the field (snapshot 1) then started forming a predefined formation (e.g., line formation). Then, the line-shaped agents reach to an environment which

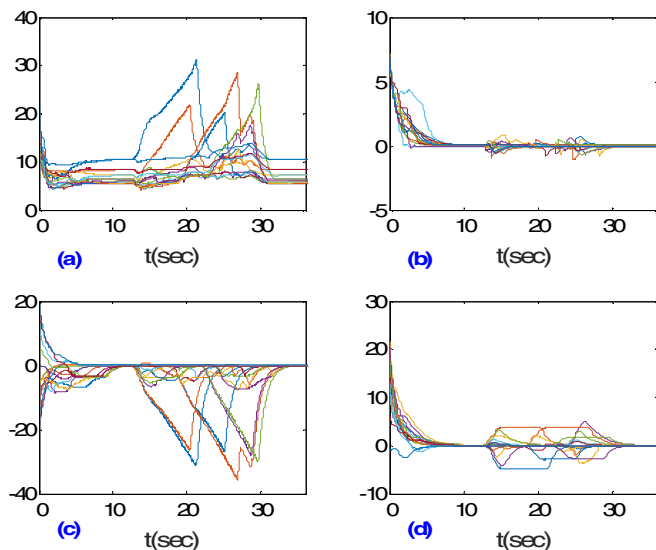


Fig. 8. (a) Distance representative  $d_{ij}^*$ ; (b) Tracking errors in the heading angles; (c) Tracking errors in the x coordinate; (d) Tracking errors in the y coordinate.

contains obstacles with different shapes, sizes and orientation angles. The agents avoid all the obstacles completely, and finally by passing the obstacles, they form a line-shape again and move to the goal. Figure 8 shows that the distance representatives of the rectangular agents converge to an equilibrium. The state errors of the agents, i.e.  $(x_i - x_{id})$ ,  $(y_i - y_{id})$ ,  $(\phi_i - \phi_{id})$  for both obstacle avoidance cases, are illustrated in Figure 8 (b, c, d). Figure 8 (b, c, d) demonstrates that the tracking errors in heading angles, x and y coordinates converge to zero before (i.e., time 0-12.5 seconds) and after (i.e., time 28-35 seconds) the obstacles have been seen by the agents and there are changing in between (i.e., time 12.5-28 seconds). This clearly shows the efficiency of the proposed obstacle avoidance algorithm.

## VI. CONCLUSIONS

This paper has presented a distributed control algorithm for multiple rectangular agents with limited communication ranges. The proposed control algorithm allows multiple agents to form a predefined formation while avoiding collision with each other. Also, by employing a potential repulsive function, the agents could be able to avoid the different shape and size obstacles. The convergence analysis of the proposed control algorithm is provided. Simulation results for the cases of line, lattice and circular formations in both free space and obstacle space have been collected to show the effectiveness of the proposed control algorithm. In the future work, we will continue to investigate other control problems of rectangular agents.

## REFERENCES

[1] R. Fierro, A. Das, J. Spletzer, J. Esposito, V. Kumar, J. P. Ostrowski, G. Pappas, C. J. Taylor, Y. Hur, R. Alur, I. Lee, G. Grudic, and B. Southall. A framework and architecture for multi-robot coordination. *Inter. J. of Robotics Research*, 21(10-11):977–995, 2002.

[2] A. Das, R. Fierro, V. Kumar, J. Ostrowski, J. Spletzer, and C. Taylor. A vision based formation control framework. *IEEE Trans. Robot. Autom.*, 18(5):813825, Oct 2002.

[3] J. Clark and R. Fierro. Mobile robotic sensors for perimeter detection and tracking. *ISA Transactions*, 46(1):3–13, 2007.

[4] H. M. La and W. Sheng. Dynamic targets tracking and observing in a mobile sensor network. *J. of Robotics and Autonomous Sys.*, 60(7):996–1009, Jul. 2012.

[5] H. M. La, R. Lim, and W. Sheng. Multi-robot cooperative learning for predator avoidance. *IEEE Trans. on Control Systems Technology*, 23(1):52–63, Jan. 2015.

[6] H. M. La and W. Sheng. Flocking control of a mobile sensor network to track and observe a moving target. *IEEE Inter. Conf. on Robotics and Automation (ICRA)*, pages 3129–3134, 2009.

[7] H. M. La and W. Sheng. Adaptive flocking control for dynamic target tracking in a mobile sensor network. *IEEE Inter. Conf. on Intell. Robots and Sys. (IROS)*, pages 4843–4848, 2009.

[8] R. Graham and J. Cortes. Spatial statistics and distributed estimation by robotic sensor networks. *American Control Conf.*, pages 2422–2427, 2010.

[9] K. M. Lynch, P. Yang, and R. A. Freeman. Decentralized environmental modeling by mobile sensor networks. *IEEE Trans. on Robotics*, 24(3):710–724, 2008.

[10] J. Cortes. Distributed Kriged Kalman filter for spatial estimation. *IEEE Trans. on Automatic Control*, 54(12):2816–2827, 2009.

[11] C. Stachniss, C. Plagemann, A. J. Lilienthal, and W. Burgard. Gas distribution modeling using sparse gaussian process mixture models. *Proc. of Robo.: Sci. and Sys.*, 2008.

[12] A. J. Lilienthal, M. Reggente, M. Trincavelli, J. L. Blanco, and J. Gonzalez. A statistical approach to gas distribution modeling with mobile robots-the kernel dm+v algorithm. *IEEE Inter. Conf. on Intell. Robot Sys.*, pages 570–576, 2009.

[13] H. M. La and W. Sheng. Distributed sensor fusion for scalar field mapping using mobile sensor networks. *IEEE Trans. on Cybernetics*, 43(2):766–778, Apr. 2013.

[14] H. M. La, W. Sheng, and J. Chen. Cooperative and active sensing in mobile sensor networks for scalar field mapping. *IEEE Trans. on Systems, Man and Cybernetics, Part A: Systems, 45(1):1–12, Jan. 2015.*

[15] H. M. La, R. S. Lim, J. Du, S. Zhang, G. Yan, and W. Sheng. Development of a small-scale research platform for intelligent transportation systems. *IEEE Trans. on Intelligent Transportation Systems*, 13(4):1753–1762, Dec. 2012.

[16] M. Egerstedt and X. Hu. Formation constrained multiagent control. *IEEE Trans. on Robotics and Automation*, 17:947951, 2001.

[17] R. Olfati-Saber. Flocking for multi-agent dynamic systems: algorithms and theory. *IEEE Trans. on Automatic Control*, 51(3):401–420, March 2006.

[18] K. D. Do. Formation control of multiple elliptical agents with limited sensing ranges. *Automatica*, 48(7):1330–1338, Jul. 2012.

[19] J. Yu and S. M. LaValle. Shortest path set induced vertex ordering and its application to distributed distance optimal formation path planning and control on graphs. In *IEEE 52nd Annual Conference on Decision and Control (CDC)*, pages 2775–2780, Dec. 2013.

[20] J. Fredslund and M. J. Matarie. A general algorithm for robot formations using local sensing and minimal communication. *IEEE Trans. on Robotics and Automation*, 18(5):837–846, Oct. 2002.

[21] H. G. Tanner, A. Jadbabaie, and G. J. Pappas. Flocking in fixed and switching networks. *IEEE Trans. on Automatic Control*, 52(5):863–868, May 2007.

[22] H. M. La and W. Sheng. Flocking control of multiple agents in noisy environments. *IEEE Inter. Conf. on Robotics and Automation (ICRA)*, pages 4964–4969, 2010.

[23] J. Hu and G. Feng. Distributed tracking control of leader-follower multi-agent systems under noisy measurement. *Automatica*, 46(8):13821387, Aug. 2010.

[24] K. D. Do. Bounded assignment formation control of second-order dynamic agents. *IEEE/ASME Transactions on Mechatronics*, 19(2):477–489, Apr. 2014.

[25] H. M. La and W. Sheng. Multi-agent motion control in cluttered and noisy environments. *J. of Communications*, 8(1):32–46, Jan. 2013.

[26] K. D. Do. Flocking for multiple elliptical agents with limited communication ranges. *IEEE Trans. on Robotics*, 27(5):931–942, Oct 2011.

- [27] K. D. Do. Formation control of underactuated ships with elliptical shape approximation and limited communication ranges. *Automatica*, 48(7):1380 – 1388, 2012.
- [28] N. Moshtagh and A. Jadbabaie. Distributed geodesic control laws for flocking of nonholonomic agents. *IEEE Trans. on Automatic Control*, 52(4):681–686, April 2007.
- [29] D. V. Dimarogonas and K. J. Kyriakopoulos. Connectedness preserving distributed swarm aggregation for multiple kinematic robots. *Robotics, IEEE Transactions on*, 24(5):1213–1223, Oct 2008.
- [30] M. M. Zavlanos, H. G. Tanner, A. Jadbabaie, and G. J. Pappas. Hybrid control for connectivity preserving flocking. *IEEE Trans. on Automatic Control*, 54(12):2869–2875, Dec. 2009.
- [31] Z. Kan, A. P. Dani, J. M. Shea, and W. E. Dixon. Network connectivity preserving formation stabilization and obstacle avoidance via a decentralized controller. *IEEE Trans. on Automatic Control*, 57(7):1827–1832, July 2012.
- [32] J. Cortes, S. Martinez, T. Karatas, and F. Bullo. Coverage control for mobile sensing networks. *IEEE Trans. on Robo. and Auto.*, 20(2):243–255, 2004.
- [33] J. Choi, S. Oh, and R. Horowitz. Distributed learning and cooperative control for multi-agent systems. *Automatica*, 45(12):2802–2814, 2009.
- [34] A. Krause, A. Singh, and C. Guestrin. Near-optimal sensor placements in gaussian processes: theory, efficient algorithms and empirical studies. *J. of Machine Learning Research*, 9:235–284, 2008.
- [35] T. Nguyen, H. M. La, and M. Jafari. On the formation control of a multi vehicle system. In *Proceedings of the ISSAT International Conference on Modeling of Complex Systems and Environments (MCSE)*, Danang-Vietnam, June 2015.
- [36] F. Zhang, D. M. Fratantoni, D. Paley, J. Lund, and N. E. Leonard. Control of coordinated patterns for ocean sampling. *Inter. J. on Control*, 80(7):1186–1199, 2007.
- [37] M. Okamoto and M. R. Akella. Avoiding the local-minimum problem in multi-agent systems with limited sensing and communication. *International Journal of Systems Science*, 0(0):1–10, Oct. 2014.
- [38] M. Okamoto and M. R. Akella. Novel potential-function-based control scheme for non-holonomic multi-agent systems to prevent the local minimum problem. *International Journal of Systems Science*, 46(12):2150–2164, 2015.
- [39] I.I. Hussein and D.M. Stipanovic. Effective coverage control for mobile sensor networks with guaranteed collision avoidance. *IEEE Trans. on Control Sys. Tech.*, 15(4):642–657, July 2007.
- [40] F. Zhang and N. E. Leonard. Cooperative filters and control for cooperative exploration. *IEEE Trans. on Automatic Control*, 55(3):650–663, 2010.
- [41] Y. Cao, W. Yu, W. Ren, and G. Chen. An overview of recent progress in the study of distributed multi-agent coordination. *IEEE Transactions on Industrial Informatics*, 9(1):427–438, Feb. 2013.
- [42] T. Fukao, H. Nakagawa, and N. Adachi. Adaptive tracking control of a nonholonomic mobile robot. *IEEE Transactions on Robotics and Automation*, 16(5):609–615, Oct 2000.
- [43] T. Nguyen and H. M. La. Formation control of multiple rectangular agents with limited communication ranges. *Advances in Visual Computing, Lecture Notes in Computer Science*, 8888:915–924, 2014.
- [44] A. Bacciotti and L. Mazzi. An invariance principle for nonlinear switched systems. *Systems & Control Letters*, 54(11):1109–1119, 2005.



**Thang Nguyen** is a Visiting Research Scholar at Cleveland State University. He received his B.Eng. and M.S. degrees from Hanoi University of Technology, Vietnam, in 2002 and 2004 respectively, and his Ph.D. degree from Rutgers University, NJ, USA, in 2010. He held positions at the University of Melbourne, the University of Leicester, the University of Exeter, and International University - Vietnam National University HCMC. His research interests include optimization, optimal control, adaptive control, sliding mode control, Atomic

Force Microscope, and Robotics.



**Hung M. La** (IEEE SM'2014, M'2009) received the B.S. and M.S. degrees in Electrical Engineering from Thai Nguyen University of Technology, Thai Nguyen, Vietnam, in 2001 and 2003, respectively, and the Ph.D. degree in Electrical and Computer Engineering from Oklahoma State University, Stillwater, OK, USA, in 2011.

He is an Assistant Professor and Director of the Advanced Robotics and Automation (ARA) Lab at the Department of Computer Science and Engineering, University of Nevada, Reno, NV, USA.

From 2011 to 2014, he was a Post Doctor and then a Research Faculty at the Center for Advanced Infrastructure and Transportation (CAIT), Rutgers University, NJ, USA. He has been actively involved in research projects with the U.S. Department of Transportation (DoT), Department of Defense (DoD), and National Science Foundation (NSF). He has authored over 50 papers published in major journals, book chapters and international conference proceedings. His current research interests include robotic systems, mobile sensor networks, cooperative control-learning-sensing systems, and intelligent transportation systems.

Dr. La is the recipient of the 2014 American Society of Civil Engineers Charles Pankow Award for the the Robotics Assisted Bridge Inspection Tool (RABIT), three best paper awards, and a best presentation award in international conferences. Dr. La is an Associate Editor of the IEEE Transactions on Human-Machine Systems, and an Editorial Board member of International Journal of Automation and Control, and International Journal of Robotic Engineering; and Guest Editor of International Journal of Robust and Nonlinear Control.



**Tuan D. Le** is a PhD student at the Advanced Robotics and Automations (ARA) Laboratory, Department of Computer Science and Engineering, University of Nevada, Reno, NV, USA. Before joining the ARA lab in 2015, he studied in Tula State University, Russia. He received his B.S. and M.S. degrees in Electrical Engineering in 2010 and 2012, respectively. His research interest includes unmanned ground robots, hybrid systems, adaptive controls, collaboration and consensus formation control.



**Mohammad Jafari** received the B.S. in Computer Hardware Engineering, Allameh Mohaddes Noori University, Iran, in 2007, and the M.S. in Mechatronics Engineering, Qazvin Islamic Azad University, Iran, in 2012. He is working toward his PhD degree at the Department of Computer Science and Engineering, University of Nevada, Reno, NV, USA. His research interests include control systems and robotics.